Discriminating the Trapped Electron Mode contribution in density fluctuation spectra

H. Arnichand[1], R. Sabot[1], S. Hacquin[1], A. Krämer-Flecken[2], C. Bourdelle[1], J. Citrin[1,3], X. Garbet[1], J.C. Giacalone[1], R. Guirlet[1], J. Hillesheim[4], L. Meneses[5], D. Villegas[1] and JET-EFDA Contributors

JET-EFDA Culham Science Centre, Abingdon, OX14 3DB, United Kingdom

[1] CEA, IRFM, F-13108 Saint-Paul-Lez-Durance, France

[2] Institute for Energy Research (Plasma Physics) Forschungszentrum Jülich, D-52425 Jülich, Germany

[3] FOM Institute DIFFER-Dutch Institute for Fundamental Energy Research, Nieuwegein, The Netherlands

[4] Culham Centre for Fusion Energy, Culham Science Centre, Abingdon, OX14 3DB, UK

[5] Instituto de Plasmas e Fusão Nuclear, Instituto Superior Técnico, Universidade Técnica de Lisboa, 1049-001 Lisboa, Portugal

E-mail: `hugo.arnichand@cea.fr`

Abstract.

Quasi-Coherent (QC) modes have been reported for more than 10 years in reflectometry fluctuations spectra in the core of tokamaks. They have characteristics in-between coherent and broadband fluctuations as they oscillate at a marked frequency but have a wide spectrum. This work presents further evidences of the link between these core QC modes and the Trapped Electron Modes (TEM) instability which has been recently established [H. Arnichand *et al.*, Nucl. Fusion **54** 123017 (2014)]. In electron cyclotron resonance heated discharges of Tore Supra, an enhancement of QC modes amplitude is observed where Nickel transport analysis and linear growth rate computations indicate that the turbulence is dominated by TEM. The disappearance of QC mode previously observed in Tore Supra and TEXTOR during density ramp-up and current ramp-down, is recovered in JET Ohmic plasmas.

Keywords: turbulence, micro-instabilities, electron cyclotron resonance heating, ohmic confinement, reflectometry

Introduction

In magnetic fusion devices, turbulent transport is attributed to long wavelength drift waves whose perpendicular wave-number $k_\perp$ normalized to the ion Larmor radius ρ_i is between $0.1 < k_\perp \rho_i < 1$. At this scale, two micro-instabilities are dominant in core tokamak plasmas: Ion Temperature Gradient (ITG) and Trapped Electron Modes (TEM) [1]. Identifying regimes where one or the other instability is predominant is essential to investigate their effects on plasma parameters and to validate turbulence models.

Although they induce a transport of the same magnitude, contributions such as the ratio q_i/q_e (ion to electron heat flux ratio) or the direction of the turbulent pinch, can be noticeably different. Due to their similar scales and comparable induced transport, discriminating these instabilities is challenging. In the plasma frame, they rotate in opposite direction but the rotation velocity of the plasma itself is usually one order of magnitude higher [2]. Discriminating ITG/TEM from particle or impurity transport requires an accurate evaluation of the diffusion coefficient and the convection velocity. Alternately, computation of the mode growth rates, based on measured plasma parameters is widely used to determine which mode is dominant [3] but it relies on theoretical predictions.

The identification of direct spectral signatures of fluctuations induced by each instability would be a noticeable progress in core physics investigations. In a recent publication [4] combining TEXTOR and Tore Supra spectra analysis, it has been evidenced that Quasi-Coherent (QC) modes shown by core reflectometry [5,6] are linked to TEM. Modifications of fluctuations spectra have been also reported during transitions toward expected TEM-dominated regimes in the plasma core of DIII-D [7, 8], Alcator C-mod [9] tokamaks, and in the MST reversed field pinch.

In several tokamak regimes (H-modes, EDA H-modes, I-mode, etc.) fluctuation spectra have shown oscillations with similar QC signatures at the very edge of the plasma. Their origins is still unclear but no link with TEM was so far established in this highly collisional plasma region. To avoid confusion, we choose to name QC-TEM the core oscillations linked with TEM that we investigate.

In this article we present a detailed analysis of Tore Supra Electron Cyclotron Resonance Heating (ECRH) plasmas and results from JET Ohmic plasmas, both supporting the link between QC modes and TEM previously evidenced [4]. Section 1 presents the diagnostics set-up and Section 2 describes the main properties of QC-TEM. In section 3, we show the ECRH effects on QC-TEM in a Tore Supra region where Nickel transport analysis and linear growth rate computation gives indications on the dominant instability. Section 4 presents reflectometry spectra in density ramp-up and current ramp-down performed in JET Ohmic plasmas, where a qualitative agreement is found with recent Tore Supra and TEXTOR observations.

	Tore Supra	TEXTOR	JET
Polarization	X-mode	O-mode	X-mode
Location in the torus	LFS	LFS and Top	LFS
Probing frequency [GHz]	100-155	26-40	75-110
Acquisition frequency [MHz]	1	2	2

Table 1. Main characteristics of the reflectometers used

1. Diagnostics set-up

This analysis uses conventional reflectometers to study density fluctuation in TEXTOR [10], Tore Supra [11] and JET [12]. Their main properties are summarized in table 1. Conventional reflectometry consists in probing the plasma with an electromagnetic wave, which is reflected at the so-called cut-off layer, and received by the reflectometer. To study density fluctuations at a given position, the probing frequency is kept constant during the time range of interest for spectral analysis. Nonetheless, to probe the plasma at different radial positions, several frequency steps are usually done within a discharge.

I-Q heterodyne systems now commonly used by reflectometers provide $A(t)cos(\phi(t))$ and $A(t)sin(\phi(t))$, where $A(t)$ and $\phi(t)$ are the amplitude and the phase, respectively. Hence, the reflectometer signal can be seen as a complex signal $A(t)e^{i\phi(t)}$. The Fourier transform of this complex signal provides spectra with positive and negative frequencies, corresponding to the phase increments and decrements respectively.

Contrary to spectra of Doppler backscattered signals [13], conventional reflectometry spectra are expected to be rather symmetric. However, a small asymmetry is always observed between positive and negative frequencies. It can arise from the combination of different phenomena (Doppler shift induced by plasma rotation, misalignment of the antenna, vertical shift of the plasma position, sawteeth, etc.) [14].

2. QC-TEM properties

2.1. Spectral signature and main characteristics

As previously introduced, in T-10 [6], TEXTOR [5] and Tore Supra [4], reflectometry fluctuation spectra can show QC-TEM oscillations ($30 < f < 150$ kHz) in different regimes. As shown in figure 1, QC modes ($\Delta f \approx f$) are in-between narrow peaks associated to coherent modes such as MHD or GAM ($\Delta f \leq f$) and broad-band fluctuations induced by turbulence ($\Delta f >> f$). They were termed Quasi-Coherent because they oscillate around a given frequency but have an intermediate status, reminiscent of broad-band fluctuations.

In TEXTOR, the several reflectometers installed at different poloidal and toroidal locations [10] allow to perform short-range poloidal correlation and long-range toroidal correlation.

Long-range toroidal correlation shows that QC-TEM modes are the only oscillations

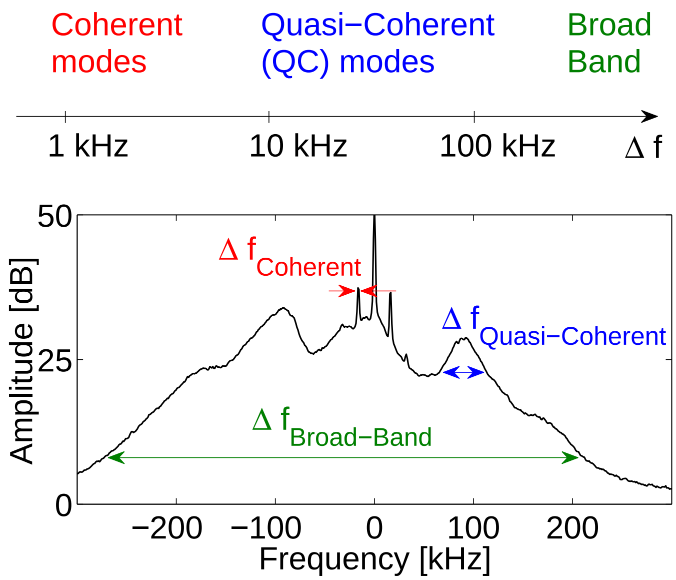

Figure 1. Example of reflectometry spectra from Tore Supra (# 40805) with its different types of component as a function of their frequency width: coherent (in red), quasi-coherent (in blue) and broad-band (in green).

which clearly appear in TEXTOR coherence spectra [15]. This has recently allowed to evidence their burst like character and their 3-dimensional nature [16].

Short-range poloidal correlation allows to estimate the perpendicular rotation. These measurements provide the total perpendicular velocity:

$$\Omega_\perp^{measured} = \Omega_\perp^{E\times B} + \Omega_\perp^{phase} \tag{1}$$

With $\Omega_\perp^{E\times B}$ the rotation due to the mean $E \times B$ drift, and $\Omega_\perp^{phase}$ the rotation due to the average phase velocity of the mode in the plasma frame. Such measurements were performed from the LFS and the top of TEXTOR. They have shown from the top of the torus only, that QC-TEM rotate faster in the electron diamagnetic direction than lower broad-band frequency fluctuations [4]. As $\Omega_\perp^{E\times B}$ is constant at a given position and time, only a distinct $\Omega_\perp^{phase}$ can explain such velocity difference (400 m/s). It suggests that $\Omega_\perp^{phase}$ is oriented in the electron diamagnetic direction for the QC modes (as expected for electron-driven modes) and/or in the ion diamagnetic direction for the low frequencies (as expected for ion-driven modes).

Short-range correlation has also provided an estimation of the poloidal wavelength associated with these QC-TEM oscillations ($0.5 < k_\perp < 3$ $[cm^{-1}]$) and their poloidal mode number ($20 < m < 70$) [5]. An estimation of their normalized scale $k_\perp \rho_i$ is also possible by using a typical ion temperature profile ($T_i\,(r/a) = T_i(0)\left[1-(r/a)^2\right]^2$), the central ion temperature $T_i(0)$ [eV] being provided by the Artsimovich's formula valid for Ohmic plasmas [17]:

$$T_i(0) = (1.29 \pm 0.11)\,\frac{(I_p \cdot B_t \cdot R^2 < n >)^{1/3}}{\sqrt{A_i}} \tag{2}$$

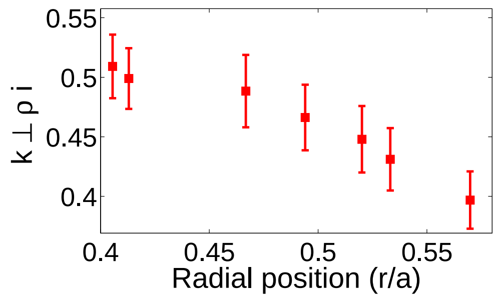

Figure 2. Normalized scale of QC-TEM estimated with equation 2 for different radial position at the LFS of TEXTOR Ohmic plasmas (#113802-7) with $B_t = 1.9$ T, $I_p = 400$ kA and $1.33 < n_e[m^{-3}10^{19}] < 1.58$.

Where I_p $[kA]$ is the plasma current, B_t $[kG]$ is the toroidal magnetic field, R $[cm]$ is the tokamak major radius, n $[10^{13}cm^{-3}]$ is the line-averaged plasma density, and A_i is the atomic mass of the working gas. Figure 2 shows the estimated values of the normalized scale of a set of Ohmic discharges of TEXTOR. It results that $k_\perp\rho_i < 0.55$, in good agreement with previous observations [5, 6]. Such normalized scale is in the range of micro-instabilities such as TEM and ITG.

2.2. Radial and poloidal location

Combining the several reflectometers installed in different tokamak, indications on the location of QC-TEM can be provided. Both poloidal and radial location of QC-TEM is in agreement with expectation for micro-instabilities:

- Radially, QC-TEM can appear at many different radial position, hence they do not depend on a specific location such as the rational surfaces or the separatrix. As an example, observations of QC-TEM have been reported in Tore Supra from $r/a \approx 0.1$ until $r/a \approx 0.8$ [4], depending on the plasma scenario.
- Poloidally, TEXTOR and Tore Supra spectra show that QC-TEM are ballooned on the Low Field Side (LFS) midplane. In TEXTOR, reflectometers can probe the plasma from the LFS midplane and from the top of the torus. Usually, more pronounced QC-TEM are observed at the LFS than at the top [figure 3(a)]. In Tore Supra, where the reflectometers are able to measure on the LFS and on the High Field Side (HFS), spectra can show QC-TEM on the LFS only [figure 3(b)].

These general properties of QC-TEM (mode number, normalized scale, radial and poloidal location, etc.) pointed toward a link with micro-instabilities. Initial investigations suggested ITG as a driving mechanism [5, 6] but this interpretation has been re-evaluated since regimes in which these modes were observed contradict this interpretation [4].

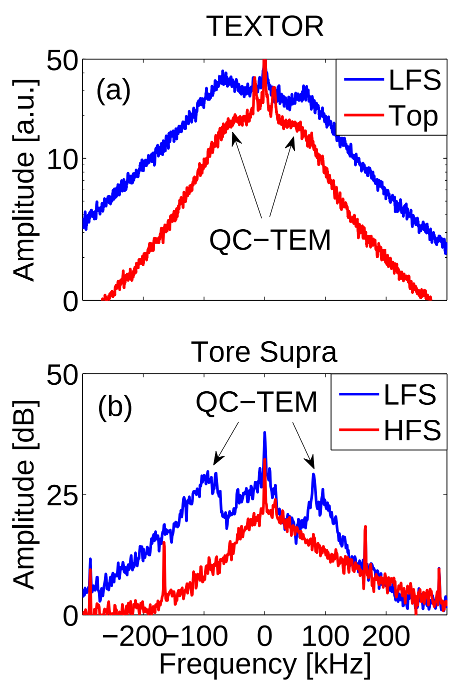

Figure 3. Poloidal ballooning of QC-TEM highlighted by reflectometry spectra from (a) TEXTOR at $r/a \approx 0.84$ between the LFS (#116492) and the top of the torus (#116495) and (b) Tore Supra between the LFS and the HFS (#40801 at $r/a \approx 0.11$).

3. QC-TEM in ECRH plasmas

ECRH has been widely used to destabilize TEM in core tokamak plasmas [7, 18–20]. Hence, its effect on QC-TEM is investigate on reflectometry fluctuation spectra of Tore Supra ($R = 2.4$ m, $a = 0.72$ m, circular plasma). A power of 250 kW of ECRH were deposited in #40801 discharges with $B_t = 3.8$ T and $I_p = 0.5$ MA. In the ECRH phase, the QC-TEM amplitude is enhanced compared to Ohmic phase [see figure 4(a)] as previously reported in T-10 [21]. In addition, a radial scan performed by changing the reflectometer frequency shows that QC-TEM are large in the core ($r/a < 0.2$), damped between $0.2 < r/a < 0.3$ and not detected further out ($r/a > 0.3$) [see figure 4(b)]. In this discharge, the ECRH power was deposited at $r/a = 0.35$.

This shot belongs to a series of discharges with Nickel injection. The deposition radii of the two gyrotrons were changed keeping the total ECRH power constant: they were either at $r/a = 0.35$ (inner deposition, as on figure 4, #40801) or at $r/a = 0.58$ (outer deposition, #40807), or one at $r/a = 0.35$ and the other one at $r/a = 0.58$ (mixed deposition, #40805). Owing to this combination, we were able to modify the temperature gradient inside $r/a = 0.3$ while keeping the density profile almost constant [22, 23]. Switching ECRH on suppresses small sawteeth observed in the Ohmic phase ($T_e < 100$ eV at the crash, inversion radius $(r/a)_{q=1} \approx 0.08$).

Nickel was injected as a trace by a laser blow-off system [24] during the ECRH phase. The impurity behavior was observed with a vacuum ultraviolet spectrometer consisting of a single line of sight in the plasma mid-plane. It measures the time evolution of the Ni XVII line at 24.92 nm, whose time evolution is used as the Ni source term in the transport simulations. Two soft-X-ray cameras with a 2 ms time resolution provide information on impurity radiation in the plasma core. Details on these diagnostics can be found in [24, 25].

The radial transport analysis of Nickel is carried out using the ITC code [24]. It solves the system of continuity equations for all the ionization stages of the injected impurity. The impurity flux for each ionization stage results from diffusion and convection:

$$\overrightarrow{\Gamma_z} = -D_z(r)\overrightarrow{\nabla} n_z(r) + \overrightarrow{V_z}(r) n_z(r) \tag{3}$$

Where $D_z(r)$ is the diffusion coefficient and $\overrightarrow{V_z}(r)$ the convection velocity. We assume that the diffusion coefficient and the convection velocity are independent of the ionization stage. Starting from an initial guess, ITC solves the system of continuity equations. It then reconstructs the VUV, bolometric and soft X-ray brightnesses. With the help of a genetic algorithm, the code converges towards the transport coefficient profiles best matching the measurements [23].

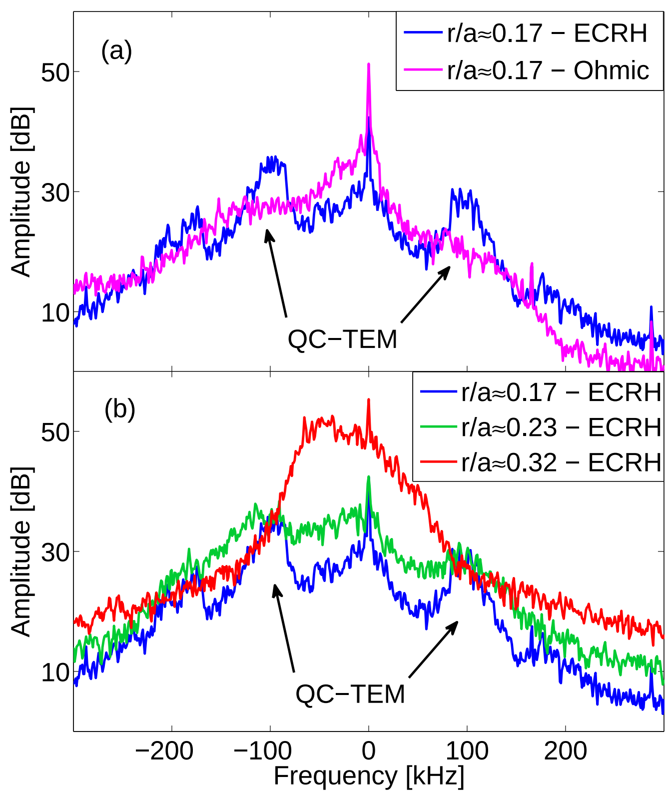

Figure 4. Fluctuation spectra of #40801 from Tore Supra reflectometry. (a) shows the difference between ECRH and Ohmic phase and (b) shows three different radial position during the ECRH phase. QC-TEM are clearly destabilized only below $r/a \approx 0.2$ in the ECRH phase.

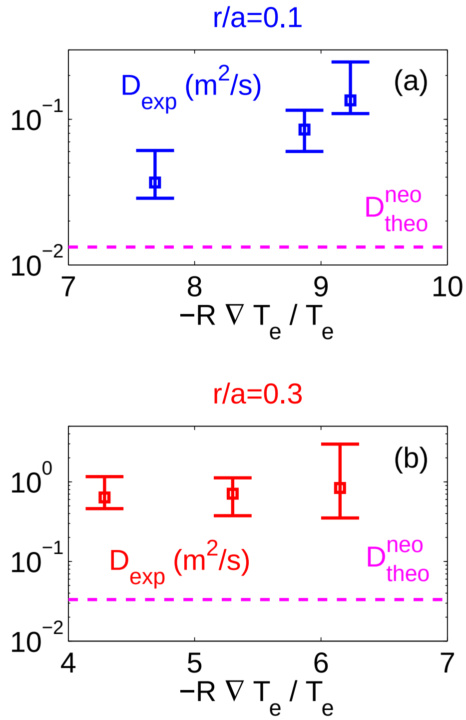

Figure 5. Experimental diffusion coefficient of nickel as a function of the normalized logarithmic electron temperature gradient at $r/a = 0.1$ (a) and $r/a = 0.3$ (b). The neoclassical diffusion coefficient is shown for both cases in dotted line

The analysis performed for the three different ECRH deposition schemes shows that the diffusion coefficient at $r/a = 0.1$ depends strongly on the normalized temperature gradient R/LT_e [figure 5(a)]. On the contrary, at $r/a = 0.3$, the diffusion coefficient is almost independent of R/LT_e [figure 5(b)].

This difference is interpreted in the frame of the theory of turbulent transport. The existence of two regions [23] are observed in linear gyrokinetic simulations [see

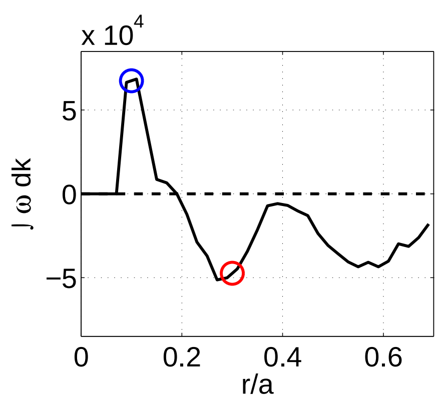

Figure 6. Radial profile of the integral over the wavenumber k of the spectrum of the most unstable mode frequency (#40801). Circles correspond to the radii at which the diffusion coefficient in shown on figure 5

figure 6] performed with the QuaLiKiz code [3]. In the core, turbulence is dominated by electron modes ($r/a < 0.15$). With TEM dominated turbulence, the transport characteristics are affected by the electron temperature hence explaining figure 5(a). Further out, ($r/a > 0.25$), ITG modes are found dominant. The fact that ITG modes are independent of the electron temperature is consistent with diffusion coefficients independent on R/LT_e [see figure 5(b)].

Thus both in terms of amplitude and radial location, observations of QC-TEM coincide with the excitation of TEM: strong QC-TEM are detected in the core ($r/a < 0.2$) where TEM are dominant. At $r/a \approx 0.3$ where QC-TEM are not observed, both the growth rate computation and the experimental Nickel diffusion coefficient indicate that turbulence is driven by ITG.

4. QC-TEM in Ohmic plasmas

In Ohmic plasmas, the confinement time first increases linearly with density in the Linear Ohmic Confinement (LOC) regime and then saturates in the Saturated Ohmic Confinement (SOC) regime, as shown in figure 7(a). Event if it still discussed [26, 27], TEM stabilization in the SOC regime is widely believed to contribute to the energy confinement saturation [2, 28–31]. The LOC-SOC transition is predicted to occur at n_s the so-called Shimomura density [32]:

$$n_s = \frac{I_p \mu_0}{2\pi a^2}\sqrt{\frac{A_i \kappa}{2}} \tag{4}$$

Where a is the minor radius of the tokamak, κ the plasma elongation, A_i the plasma atomic mass number, I_p the plasma current and μ_0 the vacuum permittivity. As shown

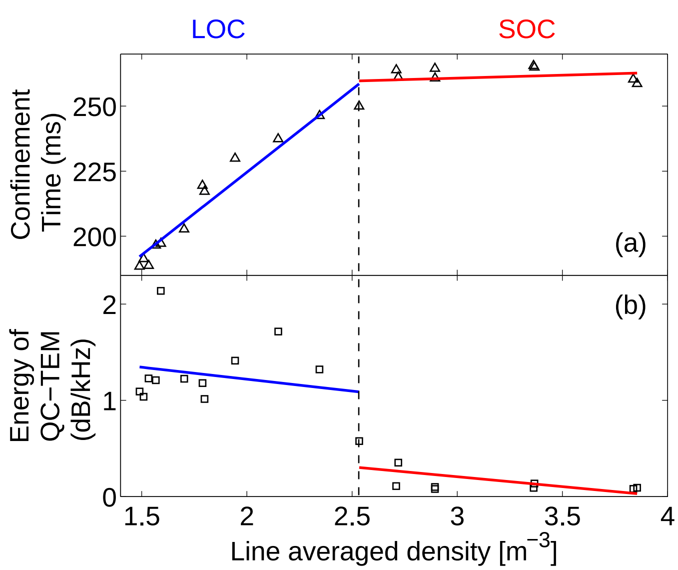

Figure 7. Confinement time (a) and energy of QC-TEM (b) as a function of the line averaged density ($B_t = 3.8$ T, $I_p = 1.2$ MA).

by equation 4, n_s is proportional to the plasma current. Hence a transition from the LOC to the SOC regimes can also be achieved at constant density with a current ramp-down. In the following chapters, both density and current scans performed in Ohmic plasmas are analyzed. One can note that equation 4 provides the plasma parameters whose depends the transition density, but that it does not allow to recover the values of the transition experimentally observed. Hence it cannot be used to determine whether the plasma is in the LOC or the SOC regime.

4.1. Stabilization of QC-TEM by density ramp-up

The advantage of performing density ramp-up to investigate the LOC-SOC transition is that the transition can be rather well identified by looking at the confinement time which saturates in the SOC regime. For reflectometry measurements, the drawback of such analysis is the modification of the cut-off layer locations during the density scan ($r/a \propto n_e$). Thus the probing frequency of the reflectometer has to be changed between each measurement to maintain a constant reflection layer in the plasma.

This was done to observe at $r/a \approx 0.3$ the evolution of QC-TEM in a set of Tore Supra discharges (#41003-41013). Figure 7(b) shows that the "energy" of QC-TEM decreases dramatically between the LOC regime (≥ 1) and the SOC regime (≤ 0.3).

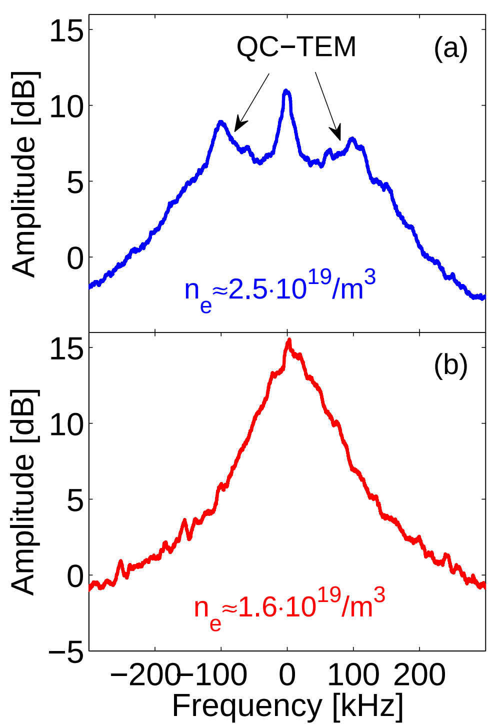

Figure 8. Fluctuation spectra from JET reflectometers KG8c measured for $0.3 < r/a < 0.33$ during #87756 ($B_t = 1.8$ T, $I_p \approx 1.8$ MA, limiter plasma). (a) shows measurements for $n_e \approx 2.5 \cdot 10^{19} m^{-3}$ with $f_{reflecto} = 86.6$ GHz and (b) for $n_e \approx 1.6 \cdot 10^{19} m^{-3}$ with $f_{reflecto} = 76.4$ GHz.

To obtain this energy, the power spectra have been decomposed in several Gaussians corresponding to each of its components (QC-TEM, broad-band, etc.). The energy of QC-TEM being defined by the ratio of the amplitude [dB] divided by the full width at half of its maximum [kHz] of the Gaussian fitting QC-TEM. Figure 7 shows that the QC-TEM stabilization and the LOC-SOC transition are strongly correlated, which support the long-standing hypothesis predicting the stabilization of TEM in the SOC regime.

A density scan ($1.5 < n_e < 2.5$) was also analyzed in JET ($R = 3.96\ m$ and $1.25 < a\ [m] < 2.10$) during an Ohmic discharge in a limited configuration (#87756). Figure 8 which presents reflectometry spectra at different densities shows that a similar picture than Tore Supra is recover in JET: QC-TEM appears only at low density. This experiment was not dedicated to the present analysis, consequently the plasma parameters make hazardous the determination of the LOC-SOC transition by confinement time estimation. Hence the comparison with Tore Supra observations (figure 7) remains qualitative.

4.2. Stabilization of QC-TEM by current ramp-down

For reflectometry measurements, performing current scan has the advantage to keep constant the measurements location during the scan. The drawback of such analysis is

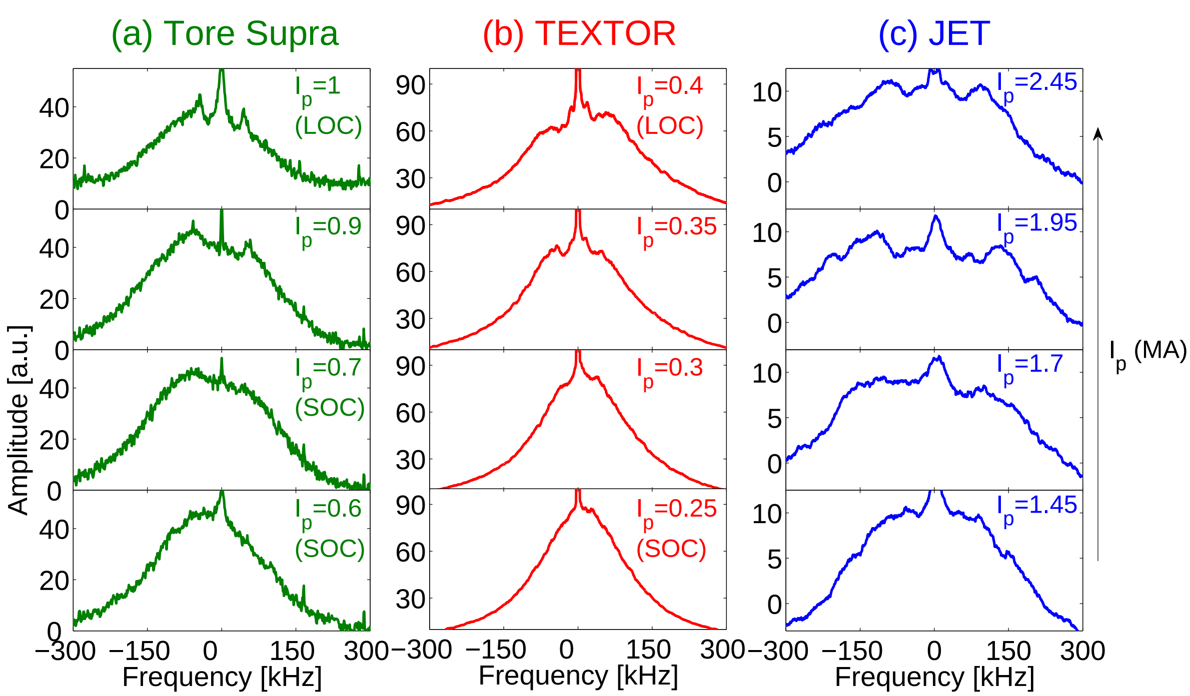

Figure 9. Reflectometry spectra from (a) Tore Supra measured at $r/a \approx 0.3$ from #40487 and #41015-41018 with $2.1 < n_e[10^{19}m^{-3}] < 2.5$, (b) TEXTOR measured at $r/a \approx 0.91$ from #117780 with $n_e \approx 3 \times 10^{19}m^{-3}$ and (c) JET measured at $0.31 < r/a < 0.43$ from #87801-2 and #87804-5 with $n_e \approx 1.65 \times 10^{19}m^{-3}$

to make more complicated the determination of the LOC-SOC transition which can be determined by:

- Using previous study related to the LOC-SOC transition. This has been done in TEXTOR [see figure 9(b)], where the transition is expected to occur at $n_e/n_{Gr} \approx 0.55$ [33] with n_{Gr} the Greenwald density ($n_{Gr} = I_p/\pi a^2$).
- Using several density scan at different plasma current to plot the transition density as a function of the plasma current. Such plot which is shown in [34], can be used to determine at which plasma current the transition will occur for a given density. This has been done for a set of Tore Supra discharges [see figure 9(a)].

Figure 9 shows that for both Tore Supra (a) and TEXTOR (b), QC-TEM observed at high current (LOC regime) disappear at low current (SOC regime). Figure 9(c) shows that a similar tendency has been found in JET where high current plasmas ($I_p = 2.45$ and 1.95 MA) show clear QC-TEM while lower plasma current show no or weak QC-TEM ($I_p = 1.45$ MA). Unfortunately, none of the two methods described above can be used in JET to determined the LOC and SOC regime in current scan. Hence the comparison between devices remains qualitative.

Conclusion and perspectives

A cross-validation between measurements and linear simulations has recently led to identify that core QC modes are linked to TEM instability [4]. In this paper we first details the main characteristics of QC-TEM which points to a link with micro-instabilities (poloidal ballooning, radial location, normalized scale, etc.). Then we show that ECRH increases QC-TEM amplitude only in a core region of Tore Supra where indications of a TEM-dominated turbulence are found in linear simulations and Nickel transport analysis. Finally, a qualitative agreement between Tore Supra, TEXTOR and JET spectra is found in Ohmic plasmas. Density ramp-up and current ramp-down show QC-TEM in low density and high current respectively, being determined as LOC regimes for Tore Supra and TEXTOR.

Recent results of non-linear simulations [35] provide indications which support the interpretation of core QC modes as a direct signature of the fluctuations induced by TEM. Indeed, TEM simulated frequency spectra exhibits a peak reminiscent of QC modes, in qualitative agreement with reflectometry frequency spectra.

The observation of QC-TEM in the plasma core combined with gyrokinetic simulations can now offer a tool to discriminate regimes where turbulence is dominated by TEM. More experimental and computational work is required to investigate the limitation of such technique. QC modes may not always be observed in TEM-dominated regimes, especially in cases of fully developped turbulence in very steep gradients plasmas.

acknowledgements

The authors thank for helpful discussions
This work, in partnership with ATEM, is financially supported by the "Conseil regional Provence-Alpes-Côte d'Azur". Its has been carried out within the framework of the Erasmus Mundus International Doctoral College in Fusion Science and Engineering (FUSION-DC) and the EUROfusion Consortium. It has received funding from the European Unions Horizon 2020 research and innovation program under grant agreement number 633053. The views and opinions expressed herein do not necessarily reflect those of the European Commission.

References

[1] X Garbet, P Mantica, C Angioni, E Asp, Y Baranov, C Bourdelle, R Budny, F Crisanti, G Cordey, L Garzotti, N Kirneva, D Hogeweij, T Hoang, F Imbeaux, E Joffrin, X Litaudon, A Manini, C McDonald, H Nordman, V Parail, A Peeters, F Ryter, C Sozzi, M Valovic, T Tala, A Thyagaraja, I Voitsekhovitch, J Weiland, H Weisen, and A Zabolotsky. *Plasma Physics and Controlled Fusion*, 46:B557, 2004.

[2] G.D. Conway, C. Angioni, R. Dux, F. Ryter, A.G. Peeters, J. Schirmer, C. Troester, CFN Reflectometry Group, and the ASDEX Upgrade team. *Nuclear Fusion*, 46(9):S799, 2006.

[3] C. Bourdelle, X. Garbet, F. Imbeaux, A. Casati, N. Dubuit, R. Guirlet, and T. Parisot. *Physics of Plasmas*, 14(11):112501, 2007.

[4] H. Arnichand, R. Sabot, S. Hacquin, A. Krämer-Flecken, X. Garbet, J. Citrin, C. Bourdelle, G. Hornung, J. Bernardo, C. Bottereau, F. Clairet, G. Falchetto, and J.C. Giacalone. Quasi-coherent modes and electron-driven turbulence. *Nuclear Fusion*, 54:123017, 2014.

[5] A. Krämer-Flecken, V. Dreval, S. Soldatov, A. Rogister, V. Vershkov, and the TEXTOR-team. *Nuclear Fusion*, 44:1143, 2004.

[6] V.A. Vershkov, D.A. Shelukhin, S.V. Soldatov, A.O. Urazbaev, S.A. Grashin, L.G. Eliseev, A.V. Melnikov, and the T-10 team. *Nuclear Fusion*, 45:S203, 2005.

[7] A. E. White, L. Schmitz, W. A. Peebles, T. L. Rhodes, T. A. Carter, G. R. McKee, M. W. Shafer, G. M. Staebler, K. H. Burrell, J. C. DeBoo, and R. Prater. *Physics of Plasma*, 17:020701, 2010.

[8] J. C. Hillesheim, J. C. DeBoo, W. A. Peebles, T. A. Carter, G. Wang, T. L. Rhodes, L. Schmitz, G. R. McKee, Z. Yan, G. M. Staebler, K. H. Burrell, E. J. Doyle, C. Holland, C. C. Petty, S. P. Smith, A. E. White, and L. Zeng. *Phys. Rev. Lett.*, 110:045003, 2013.

[9] J. E. Rice, I. Cziegler, P. H. Diamond, B. P. Duval, Y. A. Podpaly, M. L. Reinke, P. C. Ennever, M. J. Greenwald, J. W. Hughes, Y. Ma, E. S. Marmar, M. Porkolab, N. Tsujii, and S. M. Wolfe. *Phys. Rev. Lett.*, 107:265001, 2011.

[10] A. Krämer-Flecken, S. Soldatov, B. Vowinkel, and P. Mueller. *Review of Scientific Instruments*, 81:113502, 2010.

[11] R. Sabot, A. Sirinelli, J.-M. Chareau, and J.-C. Giaccalone. *Nuclear Fusion*, 46:S685, 2006.

[12] L. Cupido and L. Meneses. Recent hardware developments on synthetized sources for reflectometry hopping systems at ipfn. 11th International Reflectometry Workshop (IRW11), Ecole Polytechnique, Palaiseau, France, 2013.

[13] G D Conway, J Schirmer, S Klenge, W Suttrop, E Holzhauer, and the ASDEX Upgrade Team. Plasma rotation profile measurements using doppler reflectometry. *Plasma Physics and Controlled Fusion*, 46(6):951, 2004.

[14] G D Conway. Effects of reflectometer asymmetries on fluctuation measurements. *Plasma Physics and Controlled Fusion*, 41(1):65, 1999.

[15] A. Krämer-Flecken. In *11th International Reflectometry Workshop*, 2013.

[16] A. Krämer-Flecken. Submitted to new journal of physics.
[17] Yu. V. Gott. On artsimovichs formula. *Fizika Plazmy*, 33:958, 2007.
[18] C. Angioni, A. G. Peeters, F. Ryter, F. Jenko, G. D. Conway, T. Dannert, H. U. Fahrbach, M. Reich, W. Suttrop, and L. Fattorini. *Physics of Plasmas*, 12(4):040701, 2005.
[19] A. E. White, W. A. Peebles, T. L. Rhodes, C. H. Holland, G. Wang, L. Schmitz, T. A. Carter, J. C. Hillesheim, E. J. Doyle, L. Zeng, G. R. McKee, G. M. Staebler, R. E. Waltz, J. C. DeBoo, C. C. Petty, and K. H. Burrell. *Physics of Plasmas*, 17(5):056103, 2010.
[20] Y.J. Shi, W.H. Ko, J.M. Kwon, P.H. Diamond, S.G. Lee, S.H. Ko, L. Wang, S. Yi, K. Ida, L. Terzolo, S.W. Yoon, K.D. Lee, J.H. Lee, U.N. Nam, Y.S. Bae, Y.K. Oh, J.G. Kwak, M. Bitter, K. Hill, O.D. Gurcan, and T.S. Hahm. *Nuclear Fusion*, 53(11):113031, 2013.
[21] V.A. Vershkov, D.A. Shelukhin, M.A. Borisov, M.A. Buldakov, M.Yu. Isaev, V.P. Budaev, E.P. Gorbunov, D.S. Sergeev, T.B. Myalton, and V.V. Chistiakov. In *11th International Reflectometry Workshop*, 2013.
[22] D. Villegas, R. Guirlet, C. Bourdelle, G. T. Hoang, X. Garbet, and R. Sabot. *Phys. Rev. Lett.*, 105:035002, 2010.
[23] D. Villegas, R. Guirlet, C. Bourdelle, X. Garbet, G.T. Hoang, R. Sabot, F. Imbeaux, and J.L. Sgui. *Nuclear Fusion*, 54(7):073011, 2014.
[24] T Parisot, R Guirlet, C Bourdelle, X Garbet, N Dubuit, F Imbeaux, and P R Thomas. Experimental impurity transport and theoretical interpretation in a tore supra lower-hybrid heated plasma. *Plasma Physics and Controlled Fusion*, 50(5):055010, 2008.
[25] R. Guirlet, D. Villegas, T. Parisot, C. Bourdelle, X. Garbet, F. Imbeaux, D. Mazon, and D. Pacella. Anomalous transport of light and heavy impurities in tore supra ohmic, weakly sawtoothing plasmas. *Nuclear Fusion*, 49(5):055007, 2009.
[26] C. Sung, A.E. White, N.T. Howard, C.Y. Oi, J.E. Rice, C. Gao, P. Ennever, M. Porkolab, F. Parra, D. Mikkelsen, D. Ernst, J. Walk, J.W. Hughes, J. Irby, C. Kasten, A.E. Hubbard, M.J. Greenwald, and the Alcator C-Mod Team. *Nuclear Fusion*, 53(8):083010, 2013.
[27] R.M. McDermott, C. Angioni, G.D. Conway, R. Dux, E. Fable, R. Fischer, T. Ptterich, F. Ryter, E. Viezzer, and the ASDEX Upgrade Team. *Nuclear Fusion*, 54(4):043009, 2014.
[28] X. Garbet, J. Payan, C. Laviron, P. Devynck, S.K. Saha, H. Capes, X.P. Chen, J.P. Coulon, C. Gil, G.R. Harris, T. Hutter, A.-L. Pecquet, A. Truc, P. Hennequin, F. Gervais, and A. Quemeneur. *Nuclear Fusion*, 32(12):2147, 1992.
[29] F Wagner and U Stroth. *Plasma Physics and Controlled Fusion*, 35(10):1321, 1993.
[30] J. Candy and R.E. Waltz. *Journal of Computational Physics*, 186(2):545 – 581, 2003.
[31] C. Angioni, R. M. McDermott, F. J. Casson, E. Fable, A. Bottino, R. Dux, R. Fischer, Y. Podoba, T. Pütterich, F. Ryter, and E. Viezzer. *Phys. Rev. Lett.*, 107:215003, 2011.
[32] Y. Shimomura. *Rep. JAERI-M-85-080*, 1985.
[33] R.R. Weynants, A.M. Messiaen, J. Ongena, B. Unterberg, G. Bonheure, P. Dumortier, R. Jaspers, R. Koch, H.R. Koslowski, A. Krmer-Flecken, G. Mank, J. Rapp, M.Z. Tokar', G. Van Wassenhove, W. Biel, M. Brix, F. Durodi, G. Esser, K.H. Finken, G. Fuchs, B. Giesen, J. Hobirk, P. Httemann, M. Lehnen, A. Lyssoivan, P. Mertens, A. Pospieszczyk, U. Samm, M. Sauer, B. Schweer, R. Uhlemann, G. Van Oost, P.E. Vandenplas, M. Vervier, V. Philipps, G. Waidmann, and G.H. Wolf. *Nuclear Fusion*, 39(11Y):1637, 1999.
[34] J. E. Rice, M. J. Greenwald, Y. A. Podpaly, M. L. Reinke, P. H. Diamond, J. W. Hughes, N. T. Howard, Y. Ma, I. Cziegler, B. P. Duval, P. C. Ennever, D. Ernst, C. L. Fiore, C. Gao, J. H. Irby, E. S. Marmar, M. Porkolab, N. Tsujii, and S. M. Wolfe. *Physics of Plasmas*, 19(5):056106, 2012.
[35] J. Citrin, H. Arnichand, C. Bourdelle, J. Bernardo, X. Garbet, S. Hacquin, and R. Sabot. Progress in understanding quasi-coherent modes through gyrokinetic simulation. Joined US-EU TTF workshop, Culham, United Kingdom, 2014.